Hydrogen Deuterium Isotope Effect on Exchange Rates in η^2 Bond Transition Metal Dihydrogen Complexes Revealed by ^{2}H Solid State NMR Spectroscopy

F. Wehrmann,[†] J. Albrecht,[†] E. Gedat,[†] G. J. Kubas,[‡] J. Eckert,[‡] H.-H. Limbach,*[,†] and G. Buntkowsky*[,†]

Institut für Chemie der Freien Universität Berlin, Takustrasse 3, D-14195 Berlin, Germany, and LANSCE, Los Alamos National Laboratory, Mail Stop H805, Los Alamos, New Mexico 87545

Received: May 31, 2001; In Final Form: January 8, 2002

A selectively η^2-D_2 labeled isotopomer of the complex $W(PCy_3)_2$ $(CO)_3$) (η^2-D_2) has been synthesized and the ^{2}H NMR spectra and spin lattice relaxation rates of this complex have been measured in the temperature regime of 50 K to 300 K. The spectra have been analyzed employing a model of a combination of homonuclear dipolar D−D interaction and deuterium quadrupolar interaction and a D−D distance of 0.89 ± 0.1 Å. The line width of the spectra exhibits a weak temperature dependence at temperatures above 150 K. This temperature dependence is interpreted as a slight decrease of the quadrupolar coupling with increasing temperature, which is an indication of a change of the M−D_2 distance with changing temperatures. The spin lattice relaxation data of the complex exhibit pronounced deviations from a simple Arrhenius behavior at lower temperatures, indicating the presence of a quantum mechanical tunneling process. This process is analyzed in terms of a simple one-dimensional Bell tunnel model. A comparison with INS data from the H_2 complex reveals a strong isotope effect of 2×10^3 for the exchange rates of the deuterons.

Introduction

In the last years, a whole series of nonclassical transition metal polyhydrides with η^2-bonded dihydrogen ligands has been synthesized.[1−8] These transition metal dihydrogen complexes have very interesting physical, spectroscopic, and chemical properties, in particular, due to their short hydrogen−hydrogen distances, which vary between 0.8 and 1.7 Å and are attracting much experimental and theoretical interest.[9−29] Understanding their chemistry has led to a better understanding of catalysis because they may be catalyst precursors[20,30−32] and they can serve as stable models for short-lived intermediates in catalysis, allowing their study by NMR spectroscopy.[33]

Numerous studies[24,34−43] (and many others) have investigated the dynamic properties of the η^2-bonded dihydrogen ligands in these compounds. It is found that in many of them, the hydrogen atoms are not fixed in space as in conventional hydrogen bonds but can exchange their positions, either at higher temperatures due to conventional chemical exchange or at low temperatures due to quantum mechanical tunneling.

In general, there is a potential barrier for the exchange of the hydrogen positions. The height of the barrier is associated to the state of the two hydrogen isotopes, ranging from pure dihydrogen to pure dihydride (see Figure 1). For identical hydrogen isotopes the quantum mechanical symmetry principles have to be fulfilled and the 2-fold symmetry of the barrier causes a splitting of the energy eigenstates into states with even and odd symmetry. Thus, for a spin 1/2 particle para-states with antiparallel and ortho-states with parallel nuclear spins are formed. The height of the barrier determines the energy difference between the lowest even and odd symmetry states.

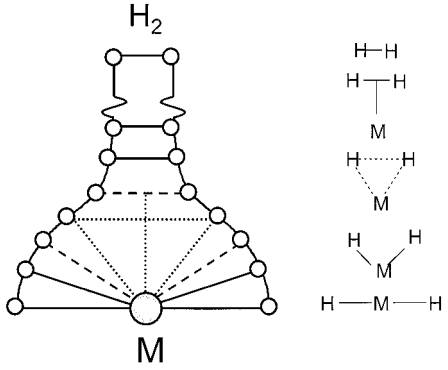

Figure 1. Sketch of a hydrogen molecule binding to a transition metal. When the H_2 or D_2 molecule becomes bound to a transition metal, different states are passed, ranging from the free hydrogen molecule over various dihydrogen states to the strongly bound dihydride. These states can be characterized by their R_{HH} or R_{MH} distance as reaction coordinate.

This energy difference is usually called tunnel splitting or tunnel frequency ν_t. The tunnel splitting depends very strongly on the hindering potential and the distance of the two hydrons. It varies from 10^{12} Hertz for dihydrogen gas to a few Hertz as the height of the potential and the distance are increased and is thus a sensitive measure of these properties.

Due to the large range of tunnel frequencies no single spectroscopic technique is able to cover the whole dynamic range. Fast coherent tunneling in the frequency range of GHz to THz has been studied by inelastic neutron scattering (INS),[24,44] and relatively slow tunneling processes in the frequency range of Hz to kHz have been investigated by ^{1}H solution NMR spectroscopy(for example, refs 24,36−41). In these ^{1}H solution NMR studies, the tunnel frequency ν_t is usually termed "quantum exchange coupling" J_{Exc}, due to the fact that for spin 1/2 particles the effect of the tunneling on the ^{1}H

* To whom all correspondence should be addressed. E-mail: bunt@chemie.fu-berlin.de.
[†] Institut für Chemie der Freien Universität Berlin.
[‡] LANSCE, Los Alamos National Laboratory.

10.1021/jp012087w CCC: $22.00 © 2002 American Chemical Society
Published on Web 03/03/2002

solution NMR spectra is equivalent to the effect of an indirect spin coupling (J-coupling).

Although similar tunnel splittings have been observed in various solid compounds with deuterated methyl groups,[45−50] which exhibit a 3-fold permutation symmetry, only recently, evidence has been found to suggest that such splittings also exist in solid dideuterium compounds.[42]

As a result of the quantum mechanical nature of the low-temperature dynamics, strong isotope effects are expected at these temperatures. Isotope effects, due to mass or spin, are common phenomena in chemical reaction dynamics and the isotopic composition of molecules affects their transformation rates.[51−54] Isotope substitution changes molecular vibration frequencies, the energy of the molecular ground state, i.e., the vibrational zero point energy, the molecular moments of inertia and the effective mass for the movement along the reaction coordinates. The quantitative analysis of these isotope effects can yield valuable information about the potential energy surface of the Hydron exchange because the rotational barrier is caused mainly by the electronic effects of the orientation of H_2 binding to the metal and to some extent also by crystal effects from neighboring molecules.

A quantitative interpretation of the dynamic processes depends strongly on the knowledge of the HH or DD distances. The difficulties of X-ray diffraction in locating hydrogen positions are the well-known. Single crystal neutron diffraction solves these difficulties, but this elaborate technique is reserved for only a few important samples where large crystals are available. As an alternative, the Hydron distances in these compounds can be determined by the analysis of magnetic dipolar interactions with solid-state NMR spectroscopy.[55,56]

The large difference in the rates is a major problem for the study of these isotope effects. In principle, this problem can be solved by a combination of ^{1}H-spin lattice relaxation measurements and ^{2}H-line shape analysis and/or ^{2}H-spin lattice relaxation. In practice, however, this would necessitate the synthesis of two labeled isotopomers, which in general is not feasible. Therefore, the combination of data from two different spectroscopic techniques with complementary dynamic ranges is necessary, for example INS data of the protonated species and NMR data of the deuterated species.

Finding a suitable compound for the search of these isotope effects is no easy task, since the synthesis of the different isotopomers must be feasible, the isotopomers must be stable and the barrier heights must be in the right range for the applied spectroscopic techniques.

The complex $W(PCy_3)_2(CO)_3(\eta^2\text{-}H_2)$, with Cy as a shortcut for -cyclohexyl ($-C_6H_{11}$), which is also known as the Kubas-complex, and its deuterated analogue $W(PCy_3)_2(CO)_3(\eta^2\text{-}D_2)$ (Figure 2), were chosen for this study for several reasons. Most importantly, the deuterated species can be prepared in a pure isotopic state from D_2 gas without the formation of other species containing unwanted W−D or C−D bonds. Experience has shown that deuteration of many other complexes leads to deuterium incorporation into C−H bonds of the ligands of the dideuterium complex. Other advantages are the high stability of the complex in the solid state under a H_2 or D_2-atmosphere, and the low cost of the synthesis.

The H_2 compound was studied by INS.[44] These data were recently reevaluated employing an Alexander-Binsch[57,58] type density matrix formalism for the description of the INS line shapes. This allowed the determination of the temperature-dependent exchange rates and the tunnel splitting of the H_2 complex.[24] In the present work, we compare the INS rate data[44] of the H_2 complex to the corresponding rate data of the D_2 complex obtained by temperature-dependent ^{2}H NMR spectroscopy and relaxometry.

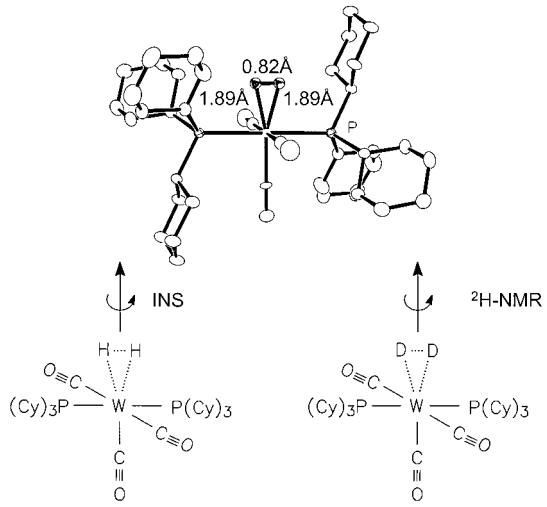

Figure 2. Upper panel: X-ray structure[71] of the tungsten complex $W(\eta^2\text{-}H_2)(CO)_3(PCy_3)_2$; Cy: = −cyclohexyl ($-C_6H_{11}$), showing the W−H and H−H distances; Lower panel: sketch of the HH and DD exchange processes, which are visible in the INS and ^{2}H NMR spectra.

This paper presents experimental evidence for the presence of a strong isotope effect on the incoherent exchange rates of solid dihydrogen complexes. Differences in the height of the corresponding energy barriers and activation energies are estimated.

The rest of this paper is organized as follows: First, a summary of sample preparations and experimental details is given. Next follows a short introduction into the theoretical background of ^{2}H NMR spectroscopy of exchanging systems and a description of the numerical methods used for calculating the spectra in the experimental section. Finally, the experimental results are presented, discussed and summarized.

Experimental Section

Spectrometer. A detailed description of our home-built three channel NMR spectrometer has been given recently.[59,60] Here, only some salient features are reproduced. All experiments were performed at a field of 6.98*T*, corresponding to a ^{2}H resonance frequency of 45.7 MHz of a standard Oxford wide bore magnet (89 mm) equipped with a room-temperature shim unit.

For the ^{2}H-channel a 2kW class AB amplifier from AMT equipped with RF-blanking for suppressing the noise during data acquisition was employed. All experiments were performed using a home-built 5 mm ^{2}H NMR probe. The probe is placed in a dynamic Oxford CF1200 helium flow cryostat. The sample temperature was controlled employing an Oxford ITC 503 temperature controller. During cooling and before and after data acquisition the sample temperature was controlled directly via a CGR-1−1000 sensor placed in the direct vicinity of the sample. This temperature was used to calibrate the readings of a second CGR-1−1000 sensor, which is part of the cryostat. During data acquisition, the first sensor was disconnected from the ITC 503 and grounded to protect the ITC from the RF and to avoid distortions of the signal. The RF was fed through a crossed diode duplexer, connected to the detection preamplifier, and through filters into the probe. The typical 90° pulse width was 3.0 μs, corresponding to a 83 kHz B_1-field in frequency units. All spectra were recorded using the solid echo technique, with an echo spacing of 30 μs. The repetition time of the

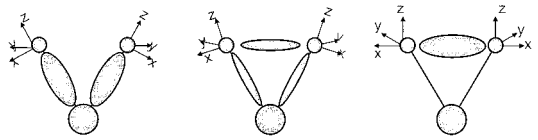

Figure 3. Sketch of quadrupolar tensor PAS system orientations and charge densities for η^2-H_2-complexes

experiments was between 5 and 400 s, depending on the T_1 relaxation time of the sample and the typical number of accumulations was 1600 scans per spectrum.

Sample Preparation. The sample of $W(PCy_3)_2(CO)_3(\eta^2\text{-}D_2)$ was prepared according to literature methods.[61]

Theory. A detailed discussion of the basic principles of coherent and incoherent tunnel exchange is given in 16, 42. The coherent and incoherent tunnel exchange at low temperatures, where only the lowest states exhibit non negligible populations, can most easily be discussed using the model of a one-dimensional hindered quantum mechanical rotor. In this model, it is assumed that the distance between the two hydrons, as well as their distance from the metal, does not change and that the angular position, described by ϕ, is the only degree of freedom.

The corresponding Schrödinger equation of a rigid rotor in a harmonic 2-fold potential is expressed as ($2V_0$ describes the depth of the hindering potential)

$$-\frac{\hbar^2}{2mr^2}\frac{d^2}{d\varphi^2}\psi - V_0(1-\cos(2\varphi))\psi = E\psi \qquad (1)$$

The solutions of this differential equation split into two branches, namely a branch of even and a branch of odd eigenfunctions.

For pairs of identical isotopes, i.e., HH (fermions) or DD (bosons), the Pauli exclusion principle must be fulfilled, i.e., the product of spatial and spin wave functions must be antisymmetric (fermions) and symmetric (bosons) under particle exchange. Due to the energy gap between the lowest two eigenstates, a tunnel splitting or exchange coupling J_{Exc}, similar to the coupling of electronic spins by the Dirac exchange interaction, appears, which is visible in NMR spectroscopy. As the result, a nuclear spin tunnel Hamiltonian which describes the splitting between adjacent states of different symmetry can be defined.

At higher temperatures, the situation becomes more complicated by two effects: On one hand higher rotational states are populated. On the NMR time scale these states are in fast exchange, leading to a thermal average of the exchange coupling and, in addition, they can also cause incoherent exchange of the two hydrons. On the other hand, the increasing centrifugal forces can lead to changes in the MH and HH (and MD and DD) distances. For a full quantum mechanical description of the system at least a two-dimensional model (rotation angle and distance) would be required. However, it was found that the empirical Bell tunneling model,[62] which describes the classical forbidden penetration of a parabolic barrier, gives surprisingly good descriptions of the incoherent kinetics in these systems.[42] This approach will also be used in this paper.

Spectra. A description of the NMR line shapes of a pair of deuterons under the influence of coherent and incoherent exchange processes has been given recently.[16] This line shape is quantitatively described in terms of a quantum-mechanical density matrix formalism, where only the nuclear spin degrees of freedom are treated quantum-mechanically.

The energy connected with the spatial degrees of freedom (the angular coordinate φ) is converted into a nuclear spin Hamiltonian (last term in eq 2) involving a coherent tunnel splitting parameter, ω_X, whereas the bath coordinates are treated via phenomenological incoherent exchange rate constants.

A homonuclear spin pair of two chemically equivalent, dipolar coupled deuteron spins **I** and **S** in a solid has a high field NMR Hamiltonian of the form

$$H = \omega_D(2I_zS_z - I_xS_x - I_yS_y) + \omega_{QS}\left(S_z^2 - \frac{2}{3}\right) + \omega_{QI}\left(I_z^2 - \frac{2}{3}\right) + \omega_X P(\mathbf{S},\mathbf{I}) \qquad (2)$$

I_k and S_k $(k = x,y,z)$ are the spin operators, ω_{QS} and ω_{QI} are the quadrupolar interactions of the two deuterons. They depend on the relative orientation of their quadrupolar tensors to the external magnetic field. The quadrupolar tensors reflect the distribution of the electronic charges and, thus, the dihydrogen state (Figure 3). ω_D is the homonuclear dipolar coupling between the I and S spins and ω_X is the tunnel splitting between the symmetric and antisymmetric spatial states. P(**S,I**) is the permutation operator of spin I and spin S. A Hilbert space base-independent definition of the permutation operator in terms of spin operators is given in the appendix. At accessible field strengths, the terms corresponding to off-resonance and chemical shift anisotropy (CSA) are at least 1 order of magnitude smaller than the above interactions and are therefore omitted. Although the coefficients of dipolar and quadrupolar interactions are functions of the orientation, the tunnel splitting is independent of the orientation.

Spin Lattice Relaxation. Besides affecting the shape of the ^{2}H NMR spectra, coherent and incoherent exchange effects also influence the ^{2}H spin lattice relaxation rates, due to the modulation of the quadrupolar interaction. Assuming that mainly the incoherent exchange will contribute to the spin lattice relaxation rate, in particular at higher temperatures, where the exchange rate will be on the order of the Zeeman-splitting of the deuterons, i.e., most efficient, the incoherent exchange rates can be determined from the spin lattice relaxation times by converting the exchange rate into a correlation time τ_c via

$$\tau_c(T) = \frac{1}{2k_{12}(T)} \qquad (3)$$

The relation between the spin lattice relaxation rate and the exchange rate depends on the motional model for the exchange process. When this type of motion is unknown, an effective coupling rate constant K^{EFG} can be used (eq 5a).[63] Several special types of motions are discussed in the literature namely: isotropic rotational diffusion (eq 5b),[64] jump motions of the deuterons (eq 5c)[65,66] (note: this eqn. is calculated from the single crystal value given in reference[66] by integration over all possible crystal orientations); axially symmetric rotational diffusion (eq 5d).[64] If $J(\tau)$ describes the spectral density function of the fluctuations

$$J(\tau) = \left[\frac{\tau}{1+(\omega_0\tau)^2} + \frac{4\tau}{1+(2\omega_0\tau)^2}\right] \qquad (4)$$

the relaxation functions are

$$\text{a}\quad \frac{1}{T_1} = K^{EFG}J(\tau)$$

$$\text{b} \quad \frac{1}{T_1} = 0.3\pi^2 q_{cc}^2 J(\tau)$$

$$\text{c} \quad \frac{1}{T_1} = \frac{9}{160}\sin^2\beta\, q_{cc}^2 J(\tau)$$

$$\text{d} \quad \frac{1}{T_1} = 0.3\pi^2 q_{cc}^2\left[\frac{1}{4}(\cos^2\beta - 1)J(\tau_0) + 3\sin^2\beta\cos^2\beta\, J(\tau_1) + \frac{3}{4}\sin^4\beta\, J(\tau^2)\right] \quad (5)$$

In these expressions τ (or τ_0, τ_1, τ_2 in case 5d) is the correlation time of the motion and β the angle between the two tensor axes (or the angle between rotation axis and tensor axis in case 5d).

The overall differences of the relaxation curves calculated with these models are relatively small on large temperature ranges, as considered in this work. For the usual spectral density function (eq 4) and an Arrhenius dependence of τ on the temperature T a single T_1 minimum and a parabolic growth of T_1 as a function of the temperature is expected. The situation changes if τ exhibits an non-Arrhenius behavior, for example due to tunneling. In this situation, eq 5a can be used to determine the exchange rates from the T_1 rates, if the position and value of the T_1 minimum are known.

Results and Discussions

Experimental Results. *^{2}H NMR Spectra.* The left part of Figure 4 presents the experimental ^{2}H NMR spectra of the W−D_2 complex, together with simulations of the spectra (see discussion). The poor S/N of the spectrum at 297 K is the result of a sensitivity problem, caused by the low deuterium concentration in the sample and the very long T_1 relaxation time at this temperature. The ^{2}H NMR spectra consist mainly of two components. The major intensity is concentrated in a rather unusual ^{2}H quadrupolar Pake pattern with an asymmetry factor of $\eta = 0.62$ and a quadrupolar interaction which slowly decreases with increasing temperature, starting from 55 kHz at 50 K to 40 kHz at 180 K. In addition, a narrow component, which accounts for less than 5% of the total spectral intensity, is present in the center of the spectrum at all temperatures. Because the sample is prepared in a D_2 atmosphere, which is in slow exchange with the η^2-bound deuterium of the complex, we attribute this narrow component to gaseous D_2 in the sample. With the exception of the small decrease of the quadrupolar interaction, visible in the line width of the spectra as a function of the temperature, the ^{2}H NMR spectrum is nearly temperature independent in the range between 50 K and 180 K.

^{2}H NMR Spin Lattice Relaxation. Figure 5 compares the experimental results of the ^{2}H NMR spin lattice relaxation measurement on the W−D_2 sample to a calculation of the spin lattice relaxation times(see below). The T_1 measurements in the temperature regime from 50 K to 230 K show a strong temperature dependence of T_1 and exhibit a typical T_1 behavior with a sharp minimum close to 110 K. At the minimum, a T_1 relaxation time of 0.78 s is found. It is evident that in the low-temperature branch of the spin lattice relaxation curve there are deviations from a simple Arrhenius behavior, visible in a flattening of the curve.

Discussion

The ^{2}H NMR spectra and spin lattice relaxation times of the Kubas W−D_2 complex have been measured in the temperature range of 50 K to 300 K. Although the ^{2}H NMR spectra reveal only a slight temperature dependence of the line shape, which corresponds to a strongly asymmetric quadrupolar tensor; the T_1 data exhibit a strong temperature dependence with a minimum at 110 K and deviations from a classical Arrhenius behavior.

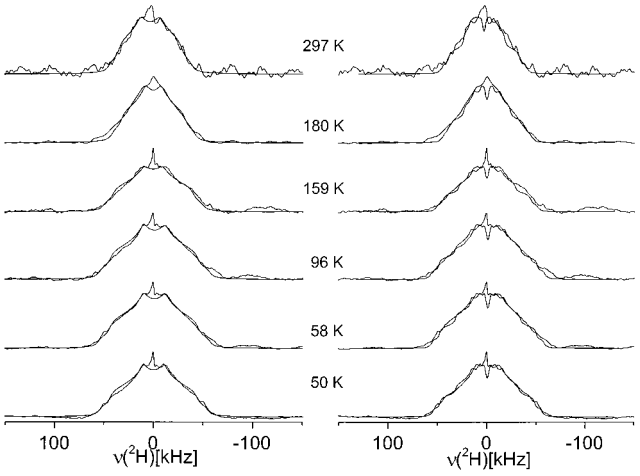

Figure 4. Experimental and simulated ^{2}H NMR spectra of the W−D_2 complex at different temperatures. Left panel: simulation as a pure quadrupolar pattern. Right panel: simulation as a superposition of a quadrupolar pattern and a homonuclear dipolar D−D interaction of 4 kHz, corresponding to a D−D distance of 0.89 Å. The latter gives clearly a better reproduction of the shoulders in the experimental line shape.

The interpretation of the ^{2}H NMR spectra was performed in two steps. First, a simulation with a simple ^{2}H Pake pattern was performed (left panel of Figure 4). This simulation gives only an unsatisfactory reproduction of the ^{2}H NMR line shape. In particular, there are shoulders in the outer parts of the ^{2}H NMR line shape, which are not explicable by a single ^{2}H Pake pattern, indicating a splitting of the lines or an impurity. Therefore, in a second step the question of the origin of these shoulders had to be solved. There are several different explanations for these shoulders:

- They can be caused by a chemical impurity,
- They can be the product of an unwanted side reaction, because of isotope fractionation, resulting in a superposition of sub spectra of the D−D and H−D isotopomer with signals of −CD groups of the rings.
- They are the result of an additional interaction in the spectra.

Chemical impurities in the sample, except the gaseous D_2 necessary for stabilizing the complex, can be excluded, due to the careful sample preparation. Isotope fractionation cannot a priori be excluded.

In this case, however, one would expect, on one hand differences in the spin lattice relaxation and the temperature dependence of the sub spectra, and, on the other hand, a slow change with time of the intensity ratios between the sub spectra, due to ongoing exchange between the gaseous D_2 and the −CH groups of the rings. Therefore, we conclude that such isotope fractionations are only of minor importance and can also be excluded as the origin of the shoulders in the spectra. In principle, there are three additional interactions which can be responsible for the shoulders in the spectra, namely coherent quantum mechanical tunneling, similar to the Ru-D_2 complex,[42] heteronuclear dipolar interactions between the ^{183}W isotope and the deuterons and homonuclear dipolar interactions between the two deuterons. Coherent quantum mechanical tunneling can be excluded in this system, because of the temperature indepen-

dence of the splitting and the fact that the much faster incoherent exchange of the two deuterons would render the coherent exchange invisible, as shown by line shape calculations.[16] Heteronuclear dipolar interactions between the ^{183}W and the deuterons are in principle capable to explain the splitting, but a splitting of ca. 4 ± 1 kHz, which is necessary to explain the line shape, corresponds to a W−D distance of 0.56 ± 0.07 Å, which is not reasonable. In the case of a homonuclear D−D interaction, a splitting of ca. 4 ± 1 kHz is estimated from the fit of the spectra, which corresponds to a D−D distance of 0.89 ± 0.1 Å. This value is in good agreement with the value of 0.89 Å found in the H_2 complex.[67] Therefore, the most probable origin of the shoulders in the spectra is the homonuclear dipolar interaction of the two deuterons. Because this interaction is invariant under exchange of the two deuterons, it is visible at all temperatures. The resulting simulations, which are shown as the right panel of Figure 4, are in good agreement with the experimental data.

It is interesting to compare this result to quantum chemical calculations of isotope effects on the dihydrogen distance by Lluch et al.[68,69] Their calculations predict that the dihydrogen complexes can be classified according to their H−H distances. For elongated complexes (> 1 Å), the potential energy curves are flat, causing strong isotope effects on the distance. This prediction was recently corroborated by Heinekey et al.,[70] who indeed found strong isotope effects on the HH/DD distance in an elongated Ru−H_2 complex. For short (<1 Å) distances however, the potential energy curves have a strong curvature, resulting in weak isotope effects. This prediction is now corroborated by our results.

For the interpretation of the minimum T_1 value, the three different models discussed above were employed, namely isotropic rotational diffusion, axially symmetric rotational diffusion and rotational jump motions between two minima. In principle, all three models are capable to reproduce the experimental data, but the values of the quadrupolar coupling constant differ strongly. For the isotropic rotational diffusion a value of $q_{cc} = 8.0$ kHz is found. The axially symmetric rotational diffusion results in a value of $q_{cc} = 7.5$ kHz. The jump exchange finally gives a value of $q_{cc} = 68$ kHz. Comparing this value to the quadrupolar coupling constant determined from the ^{2}H NMR spectra obtained at low temperatures ($q_{cc} = 4/3 \cdot 55$ kHz $= 73$ kHz), it is evident that the jump mechanism is the most probable origin of the T_1 relaxation, because only in this case the quadrupolar coupling constant obtained from the spin lattice relaxation is compatible with the value obtained from the simulation of the spectra.

For the further interpretation, the T_1 values were converted to rate constants, employing eq 4 and eq 5. The resulting rate constants are displayed in Figure 6 as a function of the inverse temperature. The resulting curve shows deviations from a simple Arrhenius behavior, visible in a concave flattening of the curve at lower temperatures. Due to the longer T_1 values at low temperatures and the correspondingly increasing measurement times we were not able to further follow the rate curve. This deviation is evidence for the presence of a quantum mechanical tunneling process at low temperatures, similar to the tunneling observed in the Ru−D_2 sample.

The observed temperature dependence of the width of the ^{2}H NMR spectra can be attributed to two different origins: on one hand the temperature-dependent exchange dynamics of the two deuterons can induce line shape changes and on the other hand, the average M−D_2 distance can change as a function of the temperature, resulting in a change of the electric field

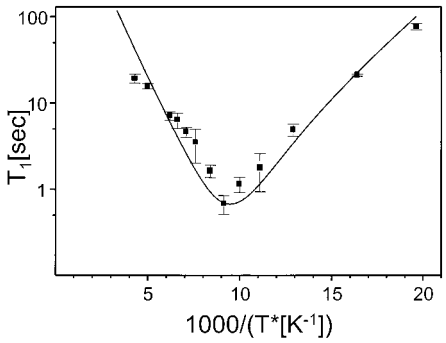

Figure 5. Experimental temperature dependence of the ^{2}H spin lattice relaxation in the W−D_2 complex. The data exhibit deviations from the Arrhenius behavior at low temperatures. The solid line is calculated from the exchange rates calculated from the Bell model.

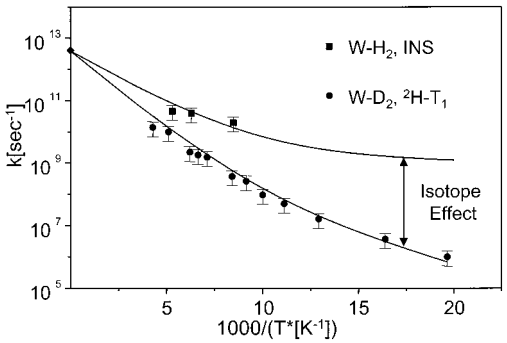

Figure 6. Arrhenius plot of the temperature dependence of the incoherent exchange rates in the W−D_2 sample, extracted from the ^{1}H− T_1 data of Figure 5. The data are compared to data obtained on the W−H_2 complex, determined by INS. The solid lines are the results of fits of the temperature dependence of the incoherent rates using a Bell type tunnel model. The fits reveal a strong isotope effect, which is not solely attributable to a simple mass effect (see text).

gradients experienced by the two deuterons. The strongest change in the width of the spectrum is observable between the 159 K spectrum and the 180 K spectrum, i.e., in a relatively narrow temperature region. In this temperature regime the incoherent exchange rates, extracted from the spin lattice relaxation, are already on the order of 10^9sec^{-1}, i.e., in the fast exchange limit, as compared to a quadrupolar coupling of ca. 50 kHz. Therefore, one can conclude that the exchange of the two deuterons is only of minor importance to the observed reduction of the width of the ^{2}H NMR spectrum and a change of the average M−D_2 distance is the more probable cause. This is a hint to the weak nature of the radial part of the potential, which shows that a full analysis of the motional dynamics of the two deuterons in the potential of the transition metal necessitates an at least two-dimensional quantum chemical calculation, which is beyond the scope of the current work.

Assuming that the spin lattice relaxation is caused by the exchange of the two deuterons, it is interesting to compare the determined D−D exchange rates to the H−H exchange rates determined from the line shape analysis of the INS spectra,[24,44] of the protonated species (upper curve in Figure 6). Due to the limited dynamic range of INS spectroscopy, compared to ^{2}H NMR, only few points in a limited temperature range are available. To enlarge this range toward high temperatures, we chose the high-temperature limit of both rates as 4×10^{12}sec^{-1}, according to the Eyring equation. A strong isotope effect is visible, which increases with lowering temperatures, approaching a value of 2×10^3 at low temperatures (Note, that without the estimation of the high temperature limit according to the Eyring equation, the weaker slope of the INS data would lead to an

even larger isotope effect at low temperatures). Calculations with the Bell tunnel model reveal that this isotope effect is not solely explainable by the difference of the mass between the two hydrogen isotopes. In the simple model of the one-dimensional hindered rotator the only alternatives are a change of either the D−D distance or a change of the activation energy. Because the D−D distance obtained from the simulation of the ^{2}H NMR spectra is in good agreement with the values measured in the protonated isotopomer, we conclude that no substantial change of the Hydron position occurs. Moreover, the quadrupolar coupling constant is practically temperature independent in the accessible temperature regime below 150 K, which means that the deuteron experiences the same field gradient at all temperatures, i.e., a constant equilibrium position. Therefore, we conclude that the major part of the observed additional isotope effect has to be attributed to a difference in the activation energy. The best fits were obtained for activation energies of $V = 69$ meV for the protonated and $V = 101$ meV for the deuterated complex, i.e., a difference of 32 meV.

In principle, this change of the activation barrier can be caused by two different reasons, which are not necessarily mutually exclusive:

•There are isotope effects on the M−D versus M−H distance, for example caused by the anharmonicity of the binding potential. As a result of these differences, the different isotopomers experience a different potential.

• The difference in the zero point energy of the ground state, and possibly also in the energy levels of an activated state which serves as the transition state for the tunneling, is responsible for the strong isotope effect.

From the NMR data it is not possible to finally distinguish between these two alternatives. However, the good agreement of the D−D distance and the H−H distance suggests that also the M−H and M−D distances are very similar. Thus, the second explanation is the more plausible explanation of the isotope effects. However, the Bell tunnel model employed in the analysis of the rate data is a simple, one-dimensional model. It neglects any multidimensional modes, for example vibrational excitations of the D−D atoms. In principle, these other modes can have significant effects on the reaction rates. Thus, a full description of the exchange kinetics can only be obtained from quantum chemical calculations of the ground and excited states on a higher theoretical level than the Bell tunnel model employed in the present analysis.

Summary and Conclusion

In summary, the ^{2}H NMR spectra and spin lattice relaxation rates of a selectively labeled W−D_2 complex have been measured in the temperature regime of 50 K to 300 K. The spectra have been analyzed employing a model of a combination of homonuclear dipolar D−D interaction and deuterium quadrupolar interaction. In the observed temperature regime, the line width of the spectra exhibits a weak temperature dependence, corresponding to a decrease of the quadrupolar coupling with increasing temperature, which is an indication of a change of the M−D_2 distance with temperature. The D−D distance coincides with the H−H distance found in the H−H complex, thus there are only minor isotope effects on the dihydrogen distance. This result corroborates quantum chemical calculations of isotope effects in dihydrogen complexes with short H−H distances by Lluch et al.[68,69]

The spin lattice relaxation data exhibit deviations from the Arrhenius behavior at low temperatures, which are an indication of the presence of a quantum mechanical tunneling process of the dideuterium pair, analogous to the H−H tunneling observed in the INS spectra of the H_2 complex. A comparison of the D−D with the H−H exchange rates, analyzed with a Bell tunneling model, reveals a strong isotope effect of 2×10^3, which is not simply explainable by the mass difference of the two hydrogen isotopes.

For a quantitative understanding of the origins of this isotope effect, an accurate evaluation of the D−D distance as a function of the temperature would be necessary. In principle such an evaluation is possible, employing a MAS technique,[56] where the ^{2}H NMR line shape of the spinning sidebands is analyzed. In the particular case of the W−D_2 complex, the application of this technique is hampered by the unstable nature of the compound, necessitating the presence of a D_2 atmosphere in the sample, which makes the preparation of a sealed sample, suitable for fast MAS spinning, very difficult.

Appendix

Base-Independent Representation of the Permutation Operator $\hat{P}(\hat{\mathbf{I}}\mathbf{I}_1, \hat{\mathbf{I}}_2)$. In our previous papers,[16,42] we used special matrix representations of the permutation operator $P(\mathbf{I}_1, \mathbf{I}_2)$, which depended on the base functions of the spin Hilbert space. Two especially convenient bases are the product base and the permutation symmetry adapted base.

In the product base of the two spins, the matrix representation of $P(\mathbf{I}_1, \mathbf{I}_2)$ can be easily calculated from

$$P(\mathbf{I}_1, \mathbf{I}_2)|\mu\nu\rangle = |\nu\mu\rangle \tag{6}$$

In the permutation symmetry adapted base, the permutation operator, $\hat{P}'(\hat{\mathbf{I}}_1, \hat{\mathbf{I}}_2)$ is diagonal, with matrix elements +1 for even (gerade) and −1 for odd (ungerade) states

$$P'(\mathbf{I}_1, \mathbf{I}_2): = (-1)^{\mu}\delta_{ij},$$
$$\mu: \text{ 0 if state } |i\rangle \text{ is gerade, 1 if ungerade} \tag{7}$$

Both definitions are equivalent and sufficient for numerical calculations. For analytical calculations or larger spin systems, however, it is advantageous to have a base-independent definition of the permutation operator in terms of spin operators. For this purpose we define the following set of normalized single spin operators:

$$\begin{bmatrix} B_1 = \frac{1}{\sqrt{2}}S_x & B_2 = \frac{1}{\sqrt{2}}S_y & B_3 = \frac{1}{\sqrt{2}}S_z \\ B_4 = \frac{1}{\sqrt{2}}E & B_5 = \frac{1}{2}\sqrt{6}\left(S_z^2 - \frac{2}{3}\right) & B_6 = \frac{1}{\sqrt{2}}(S_y^2 - S_x^2) \\ B_7 = \frac{1}{\sqrt{2}}(S_xS_y + S_yS_x) & B_8 = \frac{1}{\sqrt{2}}(S_xS_z + S_zS_x) & B_9 = \frac{1}{\sqrt{2}}(S_yS_z + S_zS_y) \end{bmatrix}$$

Employing these base operators, the permutation operator of a homo nuclear spin 1 pair is given as

$$P(\mathbf{I}_1, \mathbf{I}_2) = \sum_k B_k \otimes B_k \tag{8}$$

which can be proved by inspection.

Acknowledgment. Financial support by the Deutsche Forschungsgemeinschaft, Schwerpunktsprogramm "Zeitabhängige Phänomene und Methoden in Quantensystemen in der Physik und Chemie", is gratefully acknowledged.

References and Notes

(1) Kubas, G. J.; Ryan, R. R.; Swanson, B. I.; Vergamini, P. J.; Wasserman, H. J. *J. Am. Chem. Soc.* **1984**, *116*, 451.

(2) Kubas, G. J. *J. Acc. Chem. Res.* **1988**, *21*, 120.
(3) Jessop, P. G.; Morris, R. H. *Coord.Chem.Rev.* **1992**, *121*, 155.
(4) Heinekey, D. M.; Oldham, W. J. *J. Chem. Rev.* **1993**, *93*, 913.
(5) Sabo-Etienne, S.; Chaudret, B. *Chem. Rev.* **1998**, *98*, 2077.
(6) Luther, T. A.; Heinekey, D. M. *Inorg. Chem.* **1998**, *37*, 127.
(7) Toupadakis, A.; Kubas, G. J.; King, W. A.; Scott, L. B.; Huhmann-Vincent, J. *Organometallics* **1998**, *17*, 5315.
(8) Maltby, P. A.; Steinbeck, M.; Lough, A. J.; Morris, R. H.; Klooster, W. T.; Koetzle, T. F.; Srivastava, R. C. *J. Am. Chem. Soc.* **1996**, *118*, 5396.
(9) Aebischer, N.; Frey, U.; Merbach, A. E. *Chem. Commun.* **1998**, 2303.
(10) Albertin, G.; Antoniutti, S.; Garciafontan, S.; Carballo, R.; Padoan, F. *J. Chem. Soc., Dalton Trans.* **1998**, 2071.
(11) Alkorta, I.; Rozas, I.; Elguero, J. *Chem. Soc. Rev.* **1998**, *27*, 163.
(12) Bakhmutov, V. I. *Inorg. Chem.* **1998**, *37*, 279.
(13) Bartucz, T. Y.; Golombek, A.; Lough, A. J.; Maltby, P. A.; Morris, R. H.; Ramachandran, R.; Schlaf, M. *Inorg. Chemistry* **1998**, *37*, 1555.
(14) Basallote, M. G.; Duran, J.; Fernandez-Trujillo, M. J.; Manez, M. A. *J. Chem. Soc., Dalton Trans*. **1998**, 2205.
(15) Bohanna, C.; Callejas, B.; Edwards, A. J.; Esteruelas, M. A.; Lahoz, F. J.; Oro, L. A.; Ruiz, N.; Valero, C. *Organometallics* **1998**, *373*, 3.
(16) Buntkowsky, G.; Limbach, H.-H.; Wehrmann, F.; Sack, I.; Vieth, H. M.; Morris, R. H. *J. Phys. Chem. A* **1997**, *101*, 4679.
(17) Chaudret, B. *Coord. Chem. Rev.* **1998**, *180*, 381.
(18) Cooper, A. C.; Caulton, K. G. *Inorg. Chem.* **1998**, *37*, 5938.
(19) Crabtree, R. H. *J. Organomet. Chem.* **1998**, *557*, 111.
(20) Esteruelas, M. A.; Oro, L. A. *Chem. Rev.* **1998**, *98*, 577.
(21) Gelabert, R.; Moreno, M.; Lluch, J. M.; Lledos, A. *J. Am. Chem. Soc.* **1998**, *120*, 8168.
(22) Gründemann, S.; Limbach, H.-H.; Rodriguez, V.; Donnadieu, B.; Sabo-Etienne, S.; Chaudret, B. *Ber. Bunsen-Ges. Phys. Chem* **1998**, *102*, 344.
(23) Hasegawa, T.; Li, Z. W.; Taube, H. *Chem. Lett.* **1998**, 7.
(24) Limbach, H.-H.; Ulrich, S.; Gründemann, S.; Buntkowsky, G.; Sabo-Etienne, S.; Chaudret, B.; Kubas, G. J.; Eckert, J. *J. Am. Chem. Soc.* **1998**, *120*, 7929.
(25) Macfarlane, K. S.; Thorburn, I. S.; Cyr, P. W.; Chau, D.; Rettig, S. J.; James, B. R. *Inorg. Chim. Acta* **1998**, *270*, 130.
(26) Ng, W. S.; Jia, G. C.; Huang, M. Y.; Lau, C. P.; Wong, K. Y.; Wen, L. B. *Organometallics* **1998**, *17*, 4556.
(27) Popelier, P. L. A. *J. Phys. Chem. A* **1998**, *102*, 1873.
(28) Sabo-Etienne, S.; Chaudret, B. *Chem. Rev.* **1998**, *98*, 2077.
(29) Stahl, S. S.; Labinger, J. A.; Bercaw, J. E. *Inorg. Chem.* **1998**, *37*, 2422.
(30) Niu, S. Q.; Thomson, L. M.; Hall, M. B. *J. Am. Chem. Soc.* **1998**, *121*, 4000.
(31) Cucullu, M. E.; Nolan, S. P.; Belderrain, T. R.; Grubbs, R. H. *Organometallics* **1998**, *17*, 1299.
(32) Lough, A. J.; Morris, R. H.; Ricciuto, L.; Schleis, T. *Inorganica chimica acta* **1998**, *270*, 238.
(33) Gründemann, S.; Limbach, H.-H.; Buntkowsky, G.; Sabo-Etienne, S.; Chaudret, B. *J. Phys. Chem. A* **1999**, *103*, 4752.
(34) Limbach, H. H.; Scherer, G.; Maurer, M.; Chaudret, B. *Angew. Chem., Int. Ed. Engl.* **1990**, *31*, 1369.
(35) Limbach, H. H.; Scherer, G.; Meschede, L.; Aguilar-Parrilla, F.; Wehrle, B.; Braun, J.; Hoelger, C.; Benedict, H.; Buntkowsky, G.; Fehlhammer, W. P.; Elguero, J.; Smith, J. A. S.; Chaudret, B. *Ultrafast Reaction Dynamics and Solvent Effects, Experimental and Theoretical Aspects*; Gauduel, Y., Rossky, P. J., Eds.; American Inst. of Physics: Woodbury, NY, 1993, 225.
(36) Arliguie, T.; Chaudret, B.; Devillers, J.; Poilblanc, R. *C. R. Acad. Sci. Paris, Serie I* **1987**, *305*, 1523.
(37) Heinekey, D. M.; Payne, N. G.; Schulte, G. K. *J. Am. Chem. Soc.* **1988**, *110*, 2303.
(38) Heinekey, D. M.; Millar, J. M.; Koetzle, T. F.; Payne, N. G.; Zilm, K. W. *J. Am. Chem. Soc.* **1990**, *112*, 909.
(39) Zilm, K. W.; Heinekey, D. M.; Millar, J. M.; Payne, N. G.; Demou, P. *J. Am. Chem. Soc.* **1989**, *111*, 3088.
(40) Jones, D.; Labinger, J. A.; Weitekamp, J. *J. Am. Chem. Soc.* **1989**, *111*, 3087.
(41) Inati, S. J.; Zilm, K. W. *Phys. Rev. Lett*. **1992**, *68*, 3273.
(42) Wehrmann, F.; Fong, T.; Morris, R. H.; Limbach, H.-H.; Buntkowsky, G. *Phys. Chem. Chem. Phys.* **1999**, *1*, 4033.
(43) Facey, G. A.; Fong, T. P.; Gusev, D. G.; MacDonald, P. M.; Morris, R. H.; Schlaf, M.; Xu, W. *Can. J. Chem.* **1999**, in press.
(44) Eckert, J.; Kubas, G. J. *J. Phys. Chem.* **1993**, *97*, 2378.
(45) Lalowicz, Z. T.; Werner, U.; Müller-Warmuth, W. *Z. Naturforsch.* **1988**, *43a*, 219.
(46) Roessler, E.; Taupitz, M.; Vieth, H. M. *Ber. Bunsen-Ges.* **1989**, *93*, 1241.
(47) Bernhard, T.; Haeberlen, U. *Chem. Phys. Lett.* **1991**, *186*, 307.
(48) Detken, A.; Focke, P.; Zimmermann, H.; Haeberlen, U.; Olejniczak, Z.; Lalowicz, Z. T. *Z. Naturforsch.* **1995**, *50a*, 95.
(49) Detken, A.; Zimmermann, H. *J. Chem. Phys.* **1998**, *108*, 5845.
(50) Prager, M.; Heidemann, A. *Rotational Tunneling and Neutron Spectroscopy: A Compilation*; available from the authors, 1995.
(51) Duncan, J. F.; Cook, G. B. *Isotopes in Chemistry*; Clarendon Press: Oxford, 1968.
(52) Melander, L. *Isotope Effects on Reaction Rates*; Ronald Press: New York, 1960.
(53) Melander, L.; Saunders: W. H. *Isotopes in Chemistry*; Wiley: New York, 1980.
(54) Salikhov, K. M. *Magnetic Isotope Effect in Radical Reactions*; Springer: Wien New York, 1996.
(55) Zilm, K. W.; Merill, R. A.; Kummer, M. W.; Kubas, G. J. *J. Am. Chem. Soc.* **1986**, *108*, 7837.
(56) Facey, G.; Gusev, D.; Macholl, S.; Morris, R. H.; Buntkowsky, G. *Phys. Chem. Chem. Phys.* **2000**, *2*, 935.
(57) Alexander, S. *J. Chem. Phys.* **1962**, *37*, 971.
(58) Binsch, G. *J. Am. Chem. Soc.* **1969**, *91*, 1304.
(59) Buntkowsky, G.; Taupitz, M.; Roessler, E.; Vieth, H. M. *J. Phys. Chem. A* **1997**, *101*, 67.
(60) Gedat, E.; Schreiber, A.; Albrecht, J.; Shenderovich, I.; Findenegg, G.; Limbach, H.-H.; Buntkowsky, G. *J. Phys. Chem. B.*, submitted.
(61) Kubas, G. J.; Unkefer, C. J.; Swanson, B. I.; Fukushima, E. *J. Am. Chem. Soc.* **1986**, *108*, 7000.
(62) Bell, R. B. *The Tunnel Effect in Chemistry*; Chapman & Hall: London & NY:, 1980.
(63) Abragam, A. *Principles of Nuclear Magnetism*; Clarendon Press: Oxford, 1961.
(64) Spiess, H. W. *NMR Basic Principles and Progress*; Springer-Verlag: Berlin, Diehl, P., Fluck, E., Kosfeld, R., Eds.; 1978, *15*, 58.
(65) Benz, S.; Haeberlen, U. *J. Magn. Res.* **1986**, *66*, 125.
(66) Heuer, A.; Haeberlen, U. *J. Chem. Phys.* **1991**, *95*, 4201.
(67) Kubas, G. J.; Nelson, J. E.; Bryan, J. C.; Eckert, J.; Wisniewski, L.; Zilm, K. *Inorg. Chem.* **1994**, *33*, 2954.
(68) Torres, L.; Gelabert, R.; Moreno, M.; Lluch, J. M. *J. Phys. Chem. A* **2000**, *104*, 7898.
(69) Gelabert, R.; Moreno, M.; Lluch, J. M.; Lledós, A. *J. Am. Chem. Soc.* **1997**, *119*, 9840.
(70) Law, J. K.; Mellows, H.; Heinekey, D. M. *J. Am. Chem. Soc.* **2001**, *123*, 2085.
(71) Kubat-Martin, K. A.; Kubas, G. J.; Khaisa, G. R. K.; Van Der Sluys, L. S.; Wasserman, H. J.; Ryan, R. R., unpublished results.